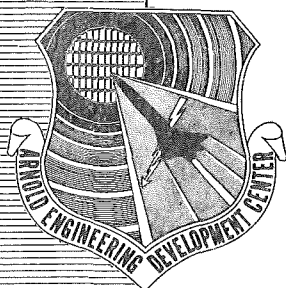# NONDIMENSIONAL CALCULATION OF TURBULENT BOUNDARY-LAYER DEVELOPMENT IN TWO-DIMENSIONAL NOZZLES OF SUPERSONIC WIND TUNNELS

By

H. Maxwell and J. L. Jacocks

Propulsion Wind Tunnel Facility

ARO, Inc.

January 1962

ARNOLD ENGINEERING DEVELOPMENT CENTER
AIR FORCE SYSTEMS COMMAND
UNITED STATES AIR FORCE

NOTICES

NONDIMENSIONAL CALCULATION OF

TURBULENT BOUNDARY-LAYER DEVELOPMENT

IN TWO-DIMENSIONAL NOZZLES

OF SUPERSONIC WIND TUNNELS

By

H. Maxwell and J. L. Jacocks

Propulsion Wind Tunnel Facility

ARO, Inc.,

a subsidiary of Sverdrup and Parcel, Inc.

January 1962

ABSTRACT

The method developed by Maurice Tucker for calculating the growth of turbulent boundary layers in two-dimensional compressible flow has been adapted to the computation of a dimensionless boundary-layer parameter. Equations and calculational procedures are presented for correcting two-dimensional supersonic nozzles for boundary-layer growth using only one or two tables, depending on the geometry. The tables are supplied for the Mach number range from 1.5 to 8.0. Agreement of calculated data with measured data and effect of Mach number distribution are shown.

CONTENTS

TABLES

ILLUSTRATIONS

NOMENCLATURE

a   Speed of sound

D   Function of Mach number, $\dfrac{7}{6}\left[\dfrac{\left(1+\frac{M^2}{5}\right)^2}{M\left(1+\frac{M^2}{10}\right)^5}\right]^{1/7}$, for $\gamma = 1.4$

$\left.\begin{array}{l}E\\I\end{array}\right\}$ Mach number functions as tabulated in Ref. 1

f   Contour scale factor

g   Ratio of displacement thickness to total thickness, δ^*/δ

H   Shape factor, δ^*/θ

K   Constant based on stagnation conditions, $0.0131\left[\dfrac{\mu_o}{\rho_o\, a_o}\right]^{1/7}$

L   Distance between nozzle throat and test section entrance

M   Mach number

N   Defined by velocity profile parameter, $\dfrac{u}{u_1} = (y/\delta)^{\frac{1}{N}}$

R_{am} $\dfrac{\rho_{am}\, u_1\, x}{\mu_{am}}$

r_T Radius of curvature of nozzle at the throat

T   Absolute temperature

u   Velocity in direction of streamline

W   One-half the distance between tunnel parallel walls

x, y   Cartesian coordinates

$\bar{x}$ Mean distance of surface interval from the effective start of the boundary-layer development

β $K \bar{\delta}_E^*$

δ Boundary-layer thickness

δ^* Boundary-layer displacement thickness

$\bar{\delta}^*$ Dimensionless boundary-layer parameter, $\delta^*/Kx_E^{6/7}$

θ Boundary-layer momentum thickness

μ Coefficient of viscosity

ρ Air density

τ Local skin-friction stress

SUBSCRIPTS

a, b	Start and end of the integration interval, respectively
am	Arithmetic mean of conditions at wall and outer edge of boundary layer
E	Exit plane of contours
i, m	Numerical indexes
L	Test section entrance
P	Perfect fluid
R	Reduced to allow for boundary-layer correction
T	Throat
TS	Test section
o	Stagnation value
1	At the outer edge of the boundary layer

INTRODUCTION

A problem that exists during both design and operation of super-
sonic wind tunnels with two-dimensional nozzles is the determination
of boundary-layer growth along the tunnel walls. Information on
boundary-layer thickness that is directly applicable to a specific tun-
nel is generally not available when design studies are initiated, and
later calculations usually are limited to a determination of the contour
correction required for a specific set of tunnel stagnation conditions.
These calculations may not easily be adapted to different stagnation
conditions or extended to regions downstream of the nozzle area. This
scarcity of information is attributed to lack of equations specifying
the growth of a turbulent boundary layer in a pressure gradient which
can be integrated in closed form. Therefore, numerical integration
is required which is time-consuming.

An effort was made to improve this situation by developing a
boundary-layer growth parameter which is independent of nozzle size
and stagnation conditions. This was accomplished by arranging the
equations of Tucker (Ref. 1) in a dimensionless form in such a way
that the coordinate along which the boundary layer develops enters into
the integration only as a ratio to the total contour length and that flow
stagnation conditions require no consideration during the integration.
Procedures were developed for reducing the dimensionless parameter
thus obtained to corrections for any contour having the same exit Mach
number and for any stagnation condition. The Mach number distribu-
tions of a representative family of contours were used in the calculation
of data which is applicable to most two-dimensional supersonic flexible
nozzles. These data and the Mach number distributions are presented.

NONDIMENSIONAL BOUNDARY-LAYER PARAMETERS

DERIVATION OF EQUATIONS

The Karman momentum-integral equation for shock-free, steady,
compressible, viscous flow

$$\tau = \frac{d}{dx} \left(\rho_1 u_1^2 \theta \right) + \rho_1 u_1 \delta^* \frac{du_1}{dx}$$

Manuscript released by authors November 1961.

was arranged by Tucker in Ref. 1 in a form suitable for numerical integration of the rate of boundary-layer development. This was accomplished by using Falkner's empirical skin-friction relationship, modified to include Mach number effects by using the density ratio ρ_{am}/ρ_1

$$\frac{\tau}{\rho_1 u_1^2} = 0.0131 \ R_{am}^{-1/7} \ (\rho_{am}/\rho_1)$$

and by specifying a constant ratio of the specific heats, $\gamma = 1.4$. Determination of the arithmetic mean temperature was simplified by assuming a Prandtl number of unity and an insulated wall, hence constant stagnation temperature throughout the flow and full temperature recovery at the wall. A further simplification was his use of the viscosity-temperature relationship $\mu_0/\mu_1 = T_0/T_1$.

Integration of the momentum-integral equation for zero pressure gradient ($du_1/dx = d\rho_1/dx = dM_1/dx = 0$), and assuming $\theta = 0$ at $x = 0$, yielded in the present notation,

$$\delta^* = K \ DH \ (x)^{6/7} \tag{1}$$

With the assumptions that N, dM_1/dx, and $x^{1/7}$ are constant for each integration interval (a, b), the momentum-integral equation was written for favorable pressure gradient as

$$\delta^*_b = (g \ E)_b \left[\frac{K \ \Delta x \ \Delta I}{\Delta M_1 \ (\bar{x})^{1/7}} + \left(\frac{\delta^*}{g \ E}\right)_a \right] \tag{2}$$

where

$$\bar{x} = \left(\frac{\delta^*}{K \ DH}\right)_a^{7/6} + \frac{\Delta x}{2} \quad \text{and} \quad \Delta(\ ) = (\ )_b - (\ )_a$$

In Tucker's work the x coordinate was measured along the contour surface, whereas for this paper, x is taken as a Cartesian coordinate. Justification of this change is shown later.

Numerical integration for the boundary-layer growth is possible by using Eq. (2) and the tabulated values of g, E, and I as given in Ref. 1. The validity of Eqs. (1) and (2) for determining supersonic nozzle corrections has been experimentally established.

The equations of Tucker are now modified to facilitate their use and to make the results more generally applicable. By writing the equations in the proper nondimensional form, it is possible to separate the effect of stagnation conditions and of nozzle sizes so that separate integrations for different situations are avoided. By dividing Eqs. (1) and (2) by the

factor K we obtain expressions which are independent of stagnation conditions. The aerodynamic contour length x_E is used as a reference length, and since the factor K has the unit of $(length)^{1/7}$, dividing both Eqs. (1) and (2) by $Kx_E^{6/7}$ yields for zero pressure gradient

$$\bar{\delta}^* = \frac{\delta^*}{Kx_E^{6/7}} = DH \left(\frac{x}{x_E}\right)^{6/7} \tag{3}$$

and for favorable pressure gradient

$$\bar{\delta}^*_b = (gE)_b \left[\frac{\frac{\Delta x}{x_E} \Delta I}{\Delta M_1 \left[\left(\frac{\bar{\delta}^*}{DH}\right)_a^{7/6} + \frac{\Delta x}{2x_E}\right]^{1/7}} + \left(\frac{\bar{\delta}^*}{gE}\right)_a \right] \tag{4}$$

The variation of $\bar{\delta}^*$ is completely determined by the variation of Mach number and of velocity profile parameter N.

PRESENTATION OF DATA

Two approximations covering the parameters upon which Eqs. (3) and (4) are dependent allow the correction of two-dimensional supersonic nozzles through the use of only one table, with a constant determined as a function of exit Mach number also required if the throat location is to be specified:

1. The extensively used velocity profile parameter N = 7 is chosen as being representative for a wide range of Reynolds numbers. Tucker gives the relation $N = 2.2 R_{am}^{1/14}$ and further states that the value for N has little effect on the calculations.

2. The wall Mach number distribution as a function of x/x_E for a given exit Mach number is considered invariant regardless of the variation in contour design procedure. Experience with several design procedures has shown this to be a reasonable approximation, especially if the contours are for flexible plates.

With these approximations the growth of the nondimensional parameter $\bar{\delta}^*$ along the contoured wall is dependent only upon the exit Mach number, M_E.

Presented in Table 1 are the distributions of the parameter $\bar{\delta}^*$ as a function of x/x_E for exit Mach numbers ranging from 1.5 to 8.0. The local Mach number distributions also are given for reference purposes, and are graphically shown in Fig. 1 as a function of x/x_E.

The frequently made assumption of zero boundary-layer thickness at the nozzle throat has not been made here. Sibulkin (Ref. 2) has given an equation which yields satisfactory throat displacement thickness. His relation has been modified to allow determination of the initial value of $\bar{\delta}*$, given by

$$\bar{\delta}*_T = \left[\frac{2\,y_T\,r_T}{x_E{}^2}\right]_P^{6/7} \tag{5}$$

where the evaluation at "P" signifies the perfect fluid contour. For a given perfect fluid contour, Eq. (5) is independent of contour scaling. The combination of parameters is a relation which is essentially a function of exit Mach number only, provided the contours are for flexible wall nozzles. Therefore Eq. (5) was used to calculate the initial values ($M_1 = 1.00$) of Table 1.

To check the effect of the approximations used in the computation of Table 1, boundary-layer measurements were made on the contoured walls of two Arnold Engineering Development Center (AEDC) wind tunnels over the Mach number range from 1.5 to 5.0. The 40-in. Supersonic Tunnel has a 40 by 40-inch test section and a flexible plate, two-dimensional nozzle, the contours of which were designed by the method of Sivells (Ref. 3). The Supersonic Model Tunnel (SMT) has a 12 by 12-inch test section and a flexible plate, two-dimensional nozzle. The SMT nozzle contours were designed using the method of characteristics and corrected for boundary-layer growth by the method presented herein. The experimentally determined displacement thicknesses were normalized to the form $\bar{\delta}*$ and transferred upstream to the aerodynamic exit planes x_E by Eq. (3) and are compared with the calculated values of $\bar{\delta}*_E$ in Fig. 2. The agreement shown in Fig. 2 justifies the assumption made previously concerning the equality of arc length and axial coordinate of the contours.

As further indication of the accuracy to be expected, two extreme deviations in Mach number distribution are given in Fig. 3, and the effect upon $\bar{\delta}*$ is shown.

For preliminary studies concerning boundary-layer growth the data given in Table 1 are sufficiently accurate. If the Mach number distribution deviation is small, then the data of Table 1 can be used for correction of perfect fluid contours for viscous effects. However, if the Mach number distribution does not closely match that used to obtain the data of Table 1, the curves of Fig. 3 should be used as a guide for adjustment of Table 1 data. The resultant flow quality is comparable to that obtainable from nozzles corrected by any of the commonly used methods.

APPLICATION TO NOZZLE CORRECTION

GENERAL PROCEDURE

The primary application of the procedure given is the correction of two-dimensional nozzle contours for viscous effects. This requires determination of the coordinates x, y of a flexible plate wall such that the aerodynamic exit coordinates x_E, y_E meet certain geometrical conditions and that the wall contour yields the desired perfect fluid flow channel when displacement thicknesses are added.

Corrections for boundary-layer thickness can be made only to the contoured surfaces of a two-dimensional flexible plate nozzle, assuming the other two walls are parallel. Hence, it is convenient to define a reduced boundary contour $(x, y)_R$ such that the assumed flow area $4y_RW$, where W is one-half the distance between the parallel walls, is equal to the effective flow area defined by using the displacement thickness δ^*. In addition, the usual simplifying assumptions are made: (1) the boundary-layer growth along the parallel walls is equal to that along the contoured walls, and (2) a cross section through the boundary layer at any station is rectangular.
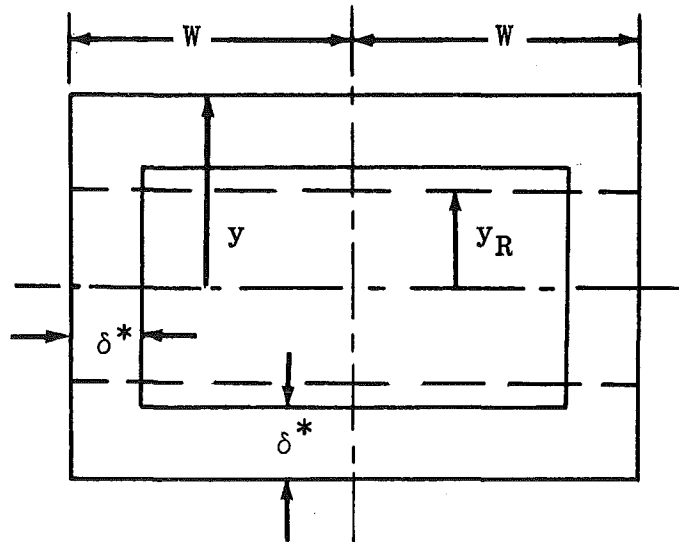
From the sketch it follows directly that the reduced ordinate is given by

$$y_R = \frac{(W - \delta^*)(y - \delta^*)}{W} \qquad (6)$$

It is necessary that an arbitrarily scaled perfect fluid design contour $(x, y)_P$ be available, and it follows that the area ratio relationship of this contour is reproduced in the reduced contour. That is, the definition

$$f = \frac{x_R}{x_P} = \frac{y_R}{y_P}$$

applies at each value of x/x_E. Since the wall contour (x, y) is to be obtained by adding a correction to y_R only, it will not be necessary to distinguish between the wall coordinate x and the reduced coordinate x_R.

Determination of the scale factor f requires consideration of Eq. (7) at the exit plane using the expression of Eq. (6) for y_R and the definition $\beta = K\bar{\delta}_E^*$

$$\left(\frac{x}{x_P}\right)_E = \frac{\left(W - \beta x_E^{6/7}\right)\left(y_E - \beta x_E^{6/7}\right)}{W y_{P_E}} = f \qquad (8)$$

Solution of Eq. (8) for x_E and f would enable determination of the physical wall coordinates

$$y = \frac{W f y_P}{W - \bar{\delta}* K x_E^{6/7}} + \bar{\delta}* K x_E^{6/7} \qquad (9)$$

$$x = f x_P$$

which are derived from Eqs. (6) and (7) and the definition for $\bar{\delta}*$.

It is necessary that the stagnation conditions contained in the parameter K be defined at this point. For a flexible wall nozzle it may be desirable to determine two or more real fluid contours to allow for large changes in the test section Reynolds number. Once the value of K is specified, then β is known since $\bar{\delta}_E^*$ is known.

Equation (8) now contains two unknowns, x_E and y_E. The manner in which y_E is found depends upon the tunnel geometry. For a flexible wall nozzle it is desirable to maintain the throat a constant distance L from the test section which has a fixed height y_{TS}. However, the aerodynamic length x_E for a family of contours is generally an increasing function of M_E. Therefore, the aerodynamic exit height y_E is generally not equal to the test section height y_{TS}.

APPLICATION TO SPECIFIC GEOMETRIES

If the distance from the throat to the test section is not specified, as would be the case for fixed-block nozzles, it can be required that $y_E = y_{TS}$. This allows solution of Eq. 8 for x_E, and the final wall contour is given by Eq. (9).

If the length L from the throat to the test section is specified, as well as the test section height, y_{TS}, further calculations are required.

It is necessary to obtain an approximate value of x_E, and thence iterate for the proper combination of x_E and y_E. There are two cases which must be considered: $x_E < L$ and $x_E > L$ with the corresponding $y_E < y_{TS}$ and $y_E > y_{TS}$. For $x_E < L$ the wall contour must be extended beyond the exit plane the distance $L - x_E$; this extension is essentially linear but its slope is dependent upon the boundary-layer growth as given by Eq. (3) and used in Eq. (9). For $x_E > L$ the aerodynamic contour is cut off the amount $x_E - L$ which yields an effective test section height of y_E. The two cases are interdependent as the converging solution may oscillate about the point $x_E = L$.

The procedure for the solution is as follows:

1. Assume an initial value of $y_{E_1} = y_{TS}$ and obtain the iterative solution of Eq. (8) for x_E.

2. If $x_E < L$, continue to Step 3a, whereas if $x_E > L$, skip to Step 3b.

3. a. $(x_E < L)$ The displacement thickness at the test section entrance is determined by using Eq. (3) written as

$$\delta^*_L = Kx_E^{6/7} (DH)_E \left[\left(\frac{\bar{\delta}^*}{(DH)} \right)_E^{7/6} + \left(\frac{L}{x_E} - 1 \right) \right]^{6/7} \tag{10}$$

The product DH is read, or interpolated, from Table 2. The values of H used to calculate Table 2 were obtained from Ref. 1 with $N = 7$ so that $DH = f(M_1)$ only. The wall ordinate at the test section entrance is now calculated:

$$y_L = \left(Wf y_{P_E} / W - \delta^*_L \right) + \delta^*_L$$

b. $(x_E > L)$ For the case of the cut-off nozzle, it is required that the aerodynamic wall contour pass through the point (L, y_{TS}). Consistency with most perfect fluid design procedures is obtained by assuming the wall contour to be made of straight-line segments in the region of the exit plane. There are two successive points on the original perfect fluid contour such that $x_{R_m} \leq L < x_{R_{m+1}}$ where $x_R = fx_P = (x/x_P)_E x_P$. Associated with each of these points of the reduced contour are the wall ordinates y_m and y_{m+1} where

$$y_m = \frac{W f y_{P_m}}{W - \bar{\delta}^*_m Kx_E^{6/7}} + \bar{\delta}^*_m Kx_E^{6/7}$$

Then, using linear interpolation, the value of y at $x = L$ is given by

$$y_L = y_m + \frac{L - x_{R_m}}{x_{R_{m+1}} - x_{R_m}} (y_{m+1} - y_m)$$

4. For either case the discrepancy between y_L and the desired value, y_{TS}, is used to obtain a corrected value of y_E

$$y_{E_{i+1}} = y_{E_i} + (y_{TS} - y_L)_i$$

Using the corrected value of y_E return to Step 1 and continue until $y_L = y_{TS}$ to within the desired accuracy.

5. For either case the final wall coordinates are given by Eq. (9) where the values of $\bar{\delta}*$ are obtained by interpolating in Table 1 as a function of x/x_E. For the case $x_E < L$ the values of $\bar{\delta}*$ for $x_E < x < L$ are found from

$$\bar{\delta}*_x = (DH)_E \left[\left(\frac{\bar{\delta}*}{\overline{DH}} \right)_E^{7/6} + \frac{x - x_E}{x_E} \right]^{6/7}$$

although this section of the wall can be made linear if $L - x_E$ is not large.

CONCLUDING REMARKS

A method for correcting two-dimensional supersonic nozzles for boundary layer which does not require integration of the rate of boundary-layer growth has been presented. The experimentally determined data presented show that corrections determined by this method are accurate for the Mach number range from 1.5 to 5. It is believed that accuracy will be comparable in the Mach number range from 5 to 8 if the nozzle walls are not cooled to such an extent as to significantly affect the ratio of displacement thickness to total thickness. With use of the tabulated data, all the effects of boundary layer on contour and nozzle design can be more accurately taken into account than by the usual approximate procedures. All the data and equations required for correcting contours and for determining the boundary-layer displacement thickness throughout the shock-free region are given in this report.

REFERENCES

1. Tucker, Maurice. "Approximate Calculation of Turbulent Boundary-
     Layer Development in Compressible Flow." NACA TN 2337,
     April 1951.

2. Sibulkin, Merwin. "Heat Transfer to an Incompressible Boundary
     Layer and Estimation of Heat-Transfer Coefficients at Super-
     sonic Nozzle Throats." Jet Propulsion Laboratory Report
     No. 20-78, July 1954.

3. Sivells, James C. "Analytic Determination of Two-Dimensional
     Supersonic Nozzle Contours Having Continuous Curvature."
     AEDC-TR-56-11, July 1956.

TABLE 1

DIMENSIONLESS BOUNDARY-LAYER PARAMETER, $\bar{\delta}*$, AS A FUNCTION
OF THE DIMENSIONLESS LONGITUDINAL COORDINATE FOR $M_E = 1.5$ TO 8.0

$\dfrac{x}{x_E}$	$M_E = 1.50$		$M_E = 1.75$		$M_E = 2.00$		$M_E = 2.25$		$\dfrac{x}{x_E}$
	M_1	$\bar{\delta}*$	M_1	$\bar{\delta}*$	M_1	$\bar{\delta}*$	M_1	$\bar{\delta}*$	
0	1.000	0.960	1.000	0.669	1.000	0.470	1.000	0.325	0
0.05	1.051	0.976	1.082	0.686	1.107	0.489	1.142	0.369	0.05
0.10	1.100	1.003	1.158	0.721	1.219	0.536	1.290	0.432	0.10
0.15	1.150	1.038	1.239	0.766	1.331	0.606	1.438	0.515	0.15
0.20	1.199	1.080	1.318	0.826	1.439	0.697	1.579	0.620	0.20
0.25	1.245	1.134	1.393	0.898	1.541	0.802	1.706	0.747	0.25
0.30	1.288	1.194	1.462	0.983	1.634	0.916	1.821	0.894	0.30
0.35	1.328	1.263	1.520	1.081	1.705	1.042	1.901	1.051	0.35
0.40	1.359	1.341	1.561	1.188	1.756	1.175	1.958	1.212	0.40
0.45	1.383	1.429	1.592	1.300	1.795	1.311	2.002	1.375	0.45
0.50	1.401	1.520	1.618	1.415	1.827	1.450	2.039	1.538	0.50
0.55	1.417	1.615	1.641	1.530	1.856	1.590	2.074	1.704	0.55
0.60	1.431	1.709	1.662	1.648	1.883	1.730	2.106	1.873	0.60
0.65	1.444	1.804	1.683	1.765	1.909	1.873	2.137	2.043	0.65
0.70	1.457	1.901	1.702	1.884	1.934	2.017	2.166	2.215	0.70
0.75	1.470	1.996	1.720	2.003	1.957	2.161	2.193	2.388	0.75
0.80	1.481	2.091	1.733	2.123	1.974	2.305	2.214	2.560	0.80
0.85	1.489	2.191	1.742	2.243	1.987	2.447	2.231	2.727	0.85
0.90	1.495	2.292	1.747	2.362	1.995	2.585	2.242	2.888	0.90
0.95	1.498	2.394	1.749	2.480	1.999	2.719	2.248	3.042	0.95
1.00	1.500	2.499	1.750	2.599	2.000	2.850	2.250	3.185	1.00

TABLE 1 (Continued)

$\dfrac{x}{x_E}$	$M_E = 2.50$		$M_E = 2.75$		$M_E = 3.00$		$M_E = 3.25$		$\dfrac{x}{x_E}$
	M_1	$\bar{\delta}^*$	M_1	$\bar{\delta}^*$	M_1	$\bar{\delta}^*$	M_1	$\bar{\delta}^*$	
0	1.000	0.219	1.000	0.140	1.000	0.080	1.000	0.048	0
0.05	1.188	0.279	1.238	0.217	1.295	0.177	1.357	0.159	0.05
0.10	1.383	0.359	1.483	0.316	1.595	0.295	1.717	0.295	0.10
0.15	1.574	0.466	1.717	0.449	1.874	0.457	2.042	0.488	0.15
0.20	1.751	0.603	1.928	0.619	2.118	0.666	2.316	0.742	0.20
0.25	1.908	0.768	2.109	0.824	2.316	0.913	2.523	1.036	0.25
0.30	2.032	0.951	2.237	1.044	2.444	1.169	2.648	1.326	0.30
0.35	2.115	1.141	2.321	1.264	2.526	1.418	2.730	1.604	0.35
0.40	2.173	1.330	2.381	1.481	2.589	1.665	2.797	1.885	0.40
0.45	2.220	1.521	2.432	1.701	2.645	1.917	2.858	2.171	0.45
0.50	2.263	1.714	2.480	1.924	2.697	2.174	2.913	2.463	0.50
0.55	2.302	1.909	2.523	2.152	2.744	2.435	2.964	2.759	0.55
0.60	2.339	2.108	2.564	2.383	2.788	2.465	3.010	3.060	0.60
0.65	2.374	2.310	2.602	2.617	2.829	2.963	3.059	3.376	0.65
0.70	2.406	2.514	2.637	2.854	2.867	3.236	3.095	3.674	0.70
0.75	2.436	2.719	2.671	3.093	2.904	3.511	3.135	3.991	0.75
0.80	2.461	2.920	2.699	3.328	2.935	3.783	3.169	4.300	0.80
0.85	2.480	3.115	2.722	3.556	2.962	4.047	3.200	4.605	0.85
0.90	2.493	3.300	2.738	3.772	2.982	4.298	3.224	4.895	0.90
0.95	2.499	3.473	2.748	3.972	2.995	4.531	3.241	5.164	0.95
1.00	2.500	3.636	2.750	4.157	3.000	4.736	3.250	5.403	1.00

TABLE 1 (Continued)

$\dfrac{x}{x_E}$	$M_E = 3.50$		$M_E = 3.75$		$M_E = 4.00$		$M_E = 4.25$		$\dfrac{x}{x_E}$
	M_1	$\bar{\delta}^*$	M_1	$\bar{\delta}^*$	M_1	$\bar{\delta}^*$	M_1	$\bar{\delta}^*$	
0	1.000	0.028	1.000	0.019	1.000	0.014	1.000	0.010	0
0.05	1.438	0.150	1.529	0.149	1.627	0.151	1.735	0.156	0.05
0.10	1.873	0.308	2.041	0.338	2.215	0.375	2.398	0.421	0.10
0.15	2.207	0.537	2.468	0.631	2.683	0.732	2.902	0.847	0.15
0.20	2.554	0.863	2.790	1.011	3.014	1.173	3.233	1.352	0.20
0.25	2.753	1.203	2.975	1.389	3.185	1.585	3.388	1.790	0.25
0.30	2.867	1.522	3.083	1.740	3.294	1.973	3.501	2.220	0.30
0.35	2.950	1.836	3.170	2.094	3.386	2.369	3.598	2.659	0.35
0.40	3.023	2.156	3.247	2.455	3.467	2.773	3.682	3.106	0.40
0.45	3.087	2.482	3.316	2.823	3.539	3.184	3.758	3.560	0.45
0.50	3.146	2.814	3.378	3.198	3.605	3.601	3.826	4.021	0.50
0.55	3.200	3.151	3.436	3.577	3.665	4.025	3.889	4.489	0.55
0.60	3.250	3.493	3.488	3.963	3.720	4.454	3.946	4.962	0.60
0.65	3.296	3.840	3.537	4.352	3.772	4.888	4.000	5.440	0.65
0.70	3.340	4.192	3.583	4.749	3.820	5.328	4.051	5.926	0.70
0.75	3.381	4.546	3.627	5.148	3.866	5.772	4.101	6.422	0.75
0.80	3.417	4.896	3.666	5.541	3.907	6.211	4.144	6.904	0.80
0.85	3.450	5.240	3.699	5.921	3.942	6.635	4.182	7.381	0.85
0.90	3.475	5.564	3.725	6.281	3.971	7.036	4.213	7.825	0.90
0.95	3.493	5.861	3.743	6.607	3.991	7.397	4.239	8.245	0.95
1.00	3.500	6.120	3.750	6.875	4.000	7.700	4.250	8.580	1.00

TABLE 1 (Continued)

$\dfrac{x}{x_E}$	$M_E = 4.50$		$M_E = 4.75$		$M_E = 5.00$		$M_E = 5.50$		$\dfrac{x}{x_E}$
	M_1	$\bar{\delta}^*$	M_1	$\bar{\delta}^*$	M_1	$\bar{\delta}^*$	M_1	$\bar{\delta}^*$	
0	1.000	0.008	1.000	0.007	1.000	0.006	1.000	0.005	0
0.05	1.881	0.170	1.984	0.180	2.119	0.194	2.374	0.229	0.05
0.10	2.625	0.496	2.815	0.562	3.006	0.641	3.386	0.829	0.10
0.15	3.159	1.010	3.389	1.171	3.596	1.334	4.009	1.708	0.15
0.20	3.458	1.555	3.643	1.727	3.851	1.942	4.238	2.382	0.20
0.25	3.606	2.028	3.795	2.242	4.006	2.506	4.406	3.054	0.25
0.30	3.723	2.504	3.919	2.766	4.135	3.079	4.545	3.734	0.30
0.35	3.823	2.990	4.025	3.300	4.244	3.662	4.664	4.423	0.35
0.40	3.911	3.484	4.118	3.843	4.340	4.253	4.768	5.120	0.40
0.45	3.990	3.986	4.200	4.393	4.426	4.852	4.861	5.824	0.45
0.50	4.061	4.494	4.275	4.951	4.503	5.457	4.945	6.534	0.50
0.55	4.126	5.009	4.344	5.515	4.574	6.069	5.021	7.252	0.55
0.60	4.186	5.530	4.408	6.085	4.640	6.687	5.092	7.975	0.60
0.65	4.242	6.055	4.467	6.660	4.701	7.311	5.158	8.703	0.65
0.70	4.295	6.589	4.522	7.241	4.758	7.940	5.220	9.437	0.70
0.75	4.346	7.128	4.576	7.840	4.812	8.575	5.278	10.177	0.75
0.80	4.392	7.665	4.625	8.431	4.863	9.215	5.334	10.924	0.80
0.85	4.431	8.181	4.669	9.009	4.909	9.842	5.387	11.678	0.85
0.90	4.464	8.671	4.708	9.571	4.949	10.446	5.435	12.420	0.90
0.95	4.490	9.119	4.736	10.064	4.982	11.009	5.475	13.113	0.95
1.00	4.500	9.471	4.750	10.468	5.000	11.466	5.500	13.667	1.00

TABLE 1 (Concluded)

$\frac{x}{x_E}$	$M_E = 6.00$		$M_E = 6.50$		$M_E = 7.00$		$M_E = 8.00$		$\frac{x}{x_E}$
	M_1	$\bar{\delta}^*$	M_1	$\bar{\delta}^*$	M_1	$\bar{\delta}^*$	M_1	$\bar{\delta}^*$	
0	1.000	0.004	1.000	0.003	1.000	0.002	1.000	0.001	0
0.05	2.723	0.290	3.014	0.357	3.411	0.468	4.132	0.736	0.05
0.10	3.837	1.102	4.220	1.388	4.703	1.805	5.559	2.722	0.10
0.15	4.439	2.147	4.823	2.605	5.234	3.101	6.014	4.208	0.15
0.20	4.671	2.936	5.067	3.540	5.488	4.148	6.296	5.549	0.20
0.25	4.849	3.724	5.258	4.443	5.688	5.192	6.516	6.875	0.25
0.30	4.996	4.520	5.413	5.357	5.853	6.239	6.700	8.196	0.30
0.35	5.121	5.322	5.547	6.283	5.994	7.289	6.858	9.516	0.35
0.40	5.232	6.132	5.665	7.214	6.120	8.344	6.997	10.835	0.40
0.45	5.330	6.948	5.770	8.150	6.231	9.403	7.122	12.156	0.45
0.50	5.420	7.770	5.866	9.092	6.333	10.467	7.236	13.482	0.50
0.55	5.502	8.598	5.953	10.040	6.425	11.534	7.340	14.809	0.55
0.60	5.578	9.432	6.034	10.991	6.511	12.604	7.435	16.132	0.60
0.65	5.648	10.271	6.109	11.948	6.591	13.683	7.525	17.468	0.65
0.70	5.714	11.115	6.180	12.910	6.666	14.764	7.609	18.804	0.70
0.75	5.776	11.965	6.247	13.878	6.737	15.847	7.688	20.137	0.75
0.80	5.835	12.823	6.310	14.855	6.805	16.949	7.764	21.495	0.80
0.85	5.889	13.667	6.370	15.837	6.867	18.037	7.836	22.843	0.85
0.90	5.938	14.486	6.425	16.799	6.923	19.086	7.901	24.155	0.90
0.95	5.977	15.240	6.471	17.694	6.971	20.069	7.957	25.388	0.95
1.00	6.000	15.845	6.500	18.394	7.000	20.847	8.000	26.434	1.00

TABLE 2

TABULATION OF VALUES OF DH AS A FUNCTION OF MACH NUMBER

| M	DH	M	DH	M	DH	M	DH
1.0	1.9905	3.0	4.4710	5.0	7.7807	7.0	11.1772
1.1	2.0626	3.1	4.6285	5.1	7.9504	7.1	11.3468
1.2	2.1426	3.2	4.7872	5.2	8.1201	7.2	11.5160
1.3	2.2307	3.3	4.9475	5.3	8.2899	7.3	11.6858
1.4	2.3256	3.4	5.1088	5.4	8.4596	7.4	11.8549
1.5	2.4276	3.5	5.2714	5.5	8.6296	7.5	12.0240
1.6	2.5350	3.6	5.4348	5.6	8.7995	7.6	12.1931
1.7	2.6486	3.7	5.5992	5.7	8.9695	7.7	12.3625
1.8	2.7670	3.8	5.7640	5.8	9.1394	7.8	12.5316
1.9	2.8905	3.9	5.9298	5.9	9.3094	7.9	12.7008
2.0	3.0180	4.0	6.0959	6.0	9.4792	8.0	12.8698
2.1	3.1500	4.1	6.2627	6.1	9.6493		
2.2	3.2855	4.2	6.4298	6.2	9.8191		
2.3	3.4246	4.3	6.5977	6.3	9.9891		
2.4	3.5665	4.4	6.7659	6.4	10.1589		
2.5	3.7116	4.5	6.9346	6.5	10.3286		
2.6	3.8590	4.6	7.1011	6.6	10.4981		
2.7	4.0090	4.7	7.2729	6.7	10.6682		
2.8	4.1611	4.8	7.4418	6.8	10.8379		
2.9	4.3152	4.9	7.6113	6.9	11.0077		
3.0	4.4710	5.0	7.7807	7.0	11.1772		
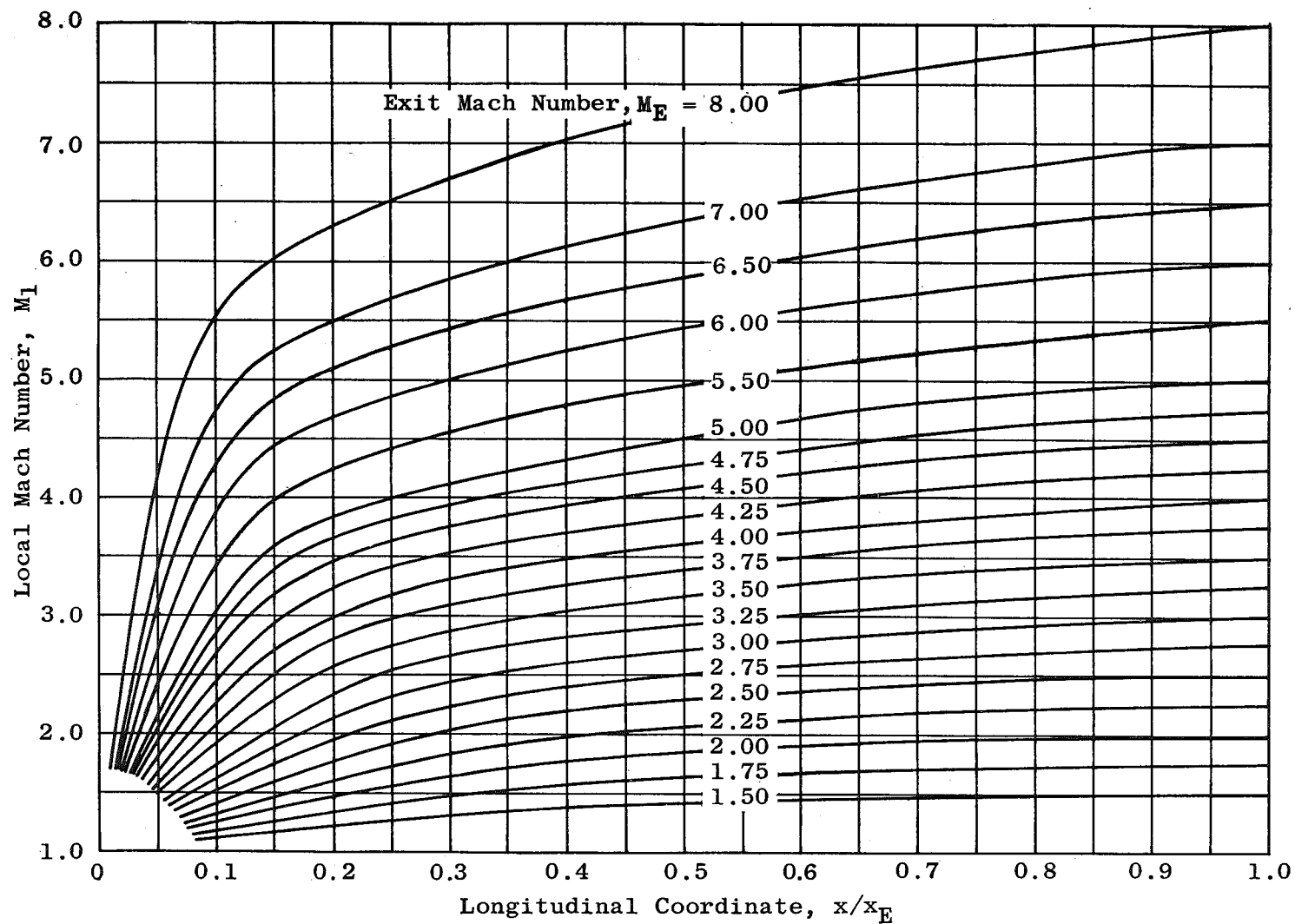
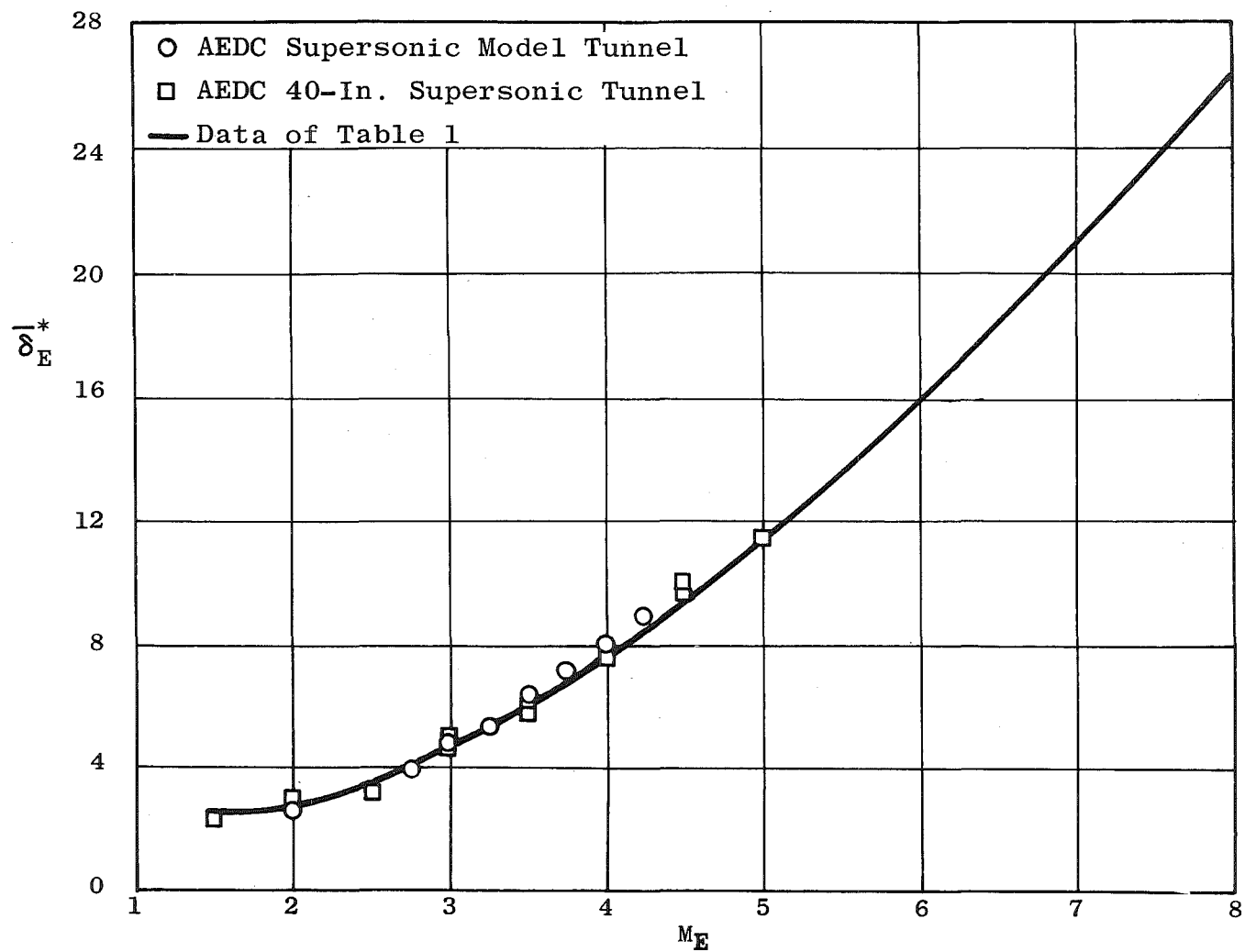Fig. 1 Mach Number Distribution as Tabulated in Table 1

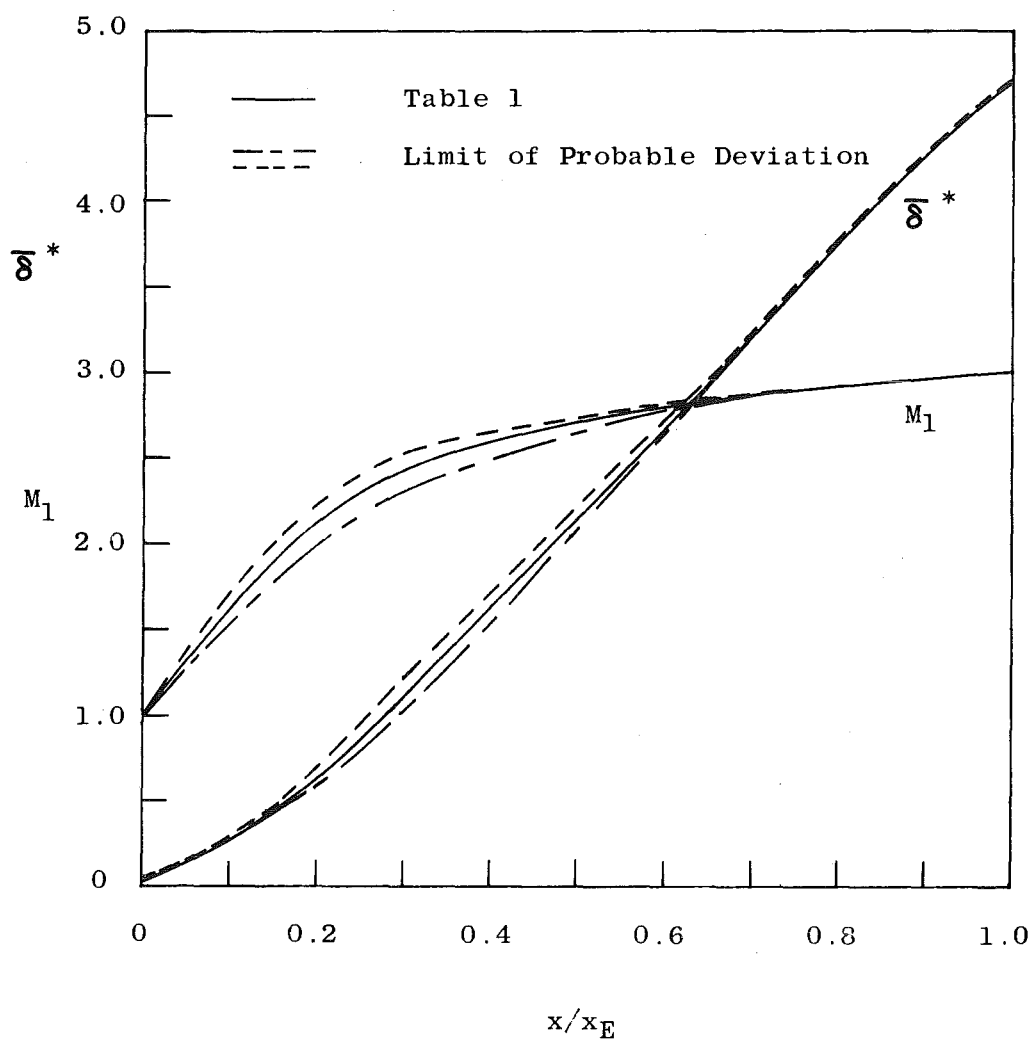Fig. 2 Comparison of Measured Data with the Exit-Plane Values of Table 1

Fig. 3 Effect of Mach Number Distribution upon $\bar{\delta}^*$ Distribution